Earth Reinforcement, Ochiai, Yasufuku & Omine (eds) © 1996 Balkema, Rotterdam. ISBN 90 5410 833 9

Bearing capacity analysis of reinforced ground

Satoru Ohtsuka, Eiji Yamada & Minoru Matsuo
Department of Geotechnical and Environmental Engineering, Nagoya University, Japan

ABSTRACT : Stability analysis of soil structure system is newly proposed which can take account of redistribution of soil structure interaction force. Two cases of soil structure systems are dealt with. One is a raft foundation and the other, a reinforced slope. The effect of mechanical properties of structures such as the rigidity and limit strength on the system stability is investigated through parametric studies. The soil structure interaction at the limit state is illustrated and discussed with the failure mode of the soil structure system.

1 INTRODUCTION

Ground reinforcement technique has been positively adopted for stabilizing soil structures in practical constructions. However, the design methods for ground reinforcement has been developed mostly based on experimental works. The slice method is so far widely used for stability assessment of reinforced soil structures. It solves equilibrium equations on sliced blocks with the assumption that the forces between blocks are at the limit state. The reinforcement effect is considered as forces working on blocks, the magnitudes of which are assumed prior to computation based on the tensile strength or the pull out resistance of reinforcements. The soil structure interaction force, however, varies with the behavior of soils and structures. It should be determined when the boundary value problem of the soil structure system is solved.

This study presents a stability analysis for soil structure system based on the shakedown theorem(Koiter, 1960). With the use of generalized stresses, the stability of soil structure system is assessed by taking account of the soil structure interaction as the internal force. Two cases of soil structure systems are dealt with in this study. One is a raft foundation and the other is a soil reinforcement with finite rigidity. They are modeled as a beam and a truss, respectively. The shakedown analysis is usually employed for the stability assessment against repeated loads. But, it is adopted here to consider the effect of mechanical properties of reinforcement on the stability. The effect of rigidity and limit strength of reinforcement on the stability will be investigated. The soil structure interaction force at the limit state will be discussed with the failure mode of reinforced slope.

2 STABILITY ANALYSIS OF SOIL STRUCTURE SYSTEM

The shakedown analysis is an expansion of the limit analysis. The feature of it is to deal with the residual stress which corresponds to the plastic strain. The residual stress is defined as the difference between the true stress $\boldsymbol{\sigma}$ and the elastic stress $\boldsymbol{\sigma}^e$ such as

$$\boldsymbol{\sigma}^r = \boldsymbol{\sigma} - \boldsymbol{\sigma}^e. \tag{2.1}$$

$\boldsymbol{\sigma}$ and $\boldsymbol{\sigma}^e$ satisfy the equilibrium equation respectively so that $\boldsymbol{\sigma}^r$ is a self-equilibrate stress. The soils and structures are modeled as the elastic perfectly plastic materials in this analysis.

2.1 *Melan's Theorem with Generalized Stresses*

The Melan's theorem assures that a soil structure system is safe against the external force $\boldsymbol{F}(t)$ if any time independent residual stress $\overline{\boldsymbol{\sigma}^r}$, $\overline{\boldsymbol{m}^r}$ can be found everywhere in the structure satisfying

$$\begin{aligned} &\boldsymbol{\sigma}^e(t) + \overline{\boldsymbol{\sigma}^r} = \boldsymbol{\sigma}^s(t), \quad f(\boldsymbol{\sigma}^s(t)) < 0 \\ &\boldsymbol{m}^e(t) + \overline{\boldsymbol{m}^r} = \boldsymbol{m}^s(t), \quad g(\boldsymbol{m}^s(t)) < 0 \end{aligned} \tag{2.2}$$

where f and g are yield functions of soils and structures, respectively. $\boldsymbol{m}$ is a generalized stress for

structures such as an axial force in a truss and a bending moment in a beam. If a structure is safe for applied load, the behavior of it is proven to shakedowns to be elastic for repeat of load.

2.2 *Shakedown Analysis with Linear Programming*

The Melan's theorem gives a lower bound for the exact solution on the stability so that it is formulated as a maximization problem(Maier,1969). When the external force is a monotonically increasing force, the Melan's theorem coincides with the lower bound theorem in the limit analysis. With the use of linear yield functions, Eq.(2.2) is described as follows:

$$N^T \left\{ \begin{array}{c} \boldsymbol{\sigma} \\ \boldsymbol{m} \end{array} \right\} - \boldsymbol{K} = N^T \left(\left\{ \begin{array}{c} \boldsymbol{\sigma}_o \\ \boldsymbol{m}_o \end{array} \right\} + \left\{ \begin{array}{c} \boldsymbol{\sigma}^e \\ \boldsymbol{m}^e \end{array} \right\} + \left\{ \begin{array}{c} \overline{\boldsymbol{\sigma}}^r \\ \overline{\boldsymbol{m}}^r \end{array} \right\} \right) - \boldsymbol{K} \leq \mathbf{o} \tag{2.3}$$

The finite discretization on stresses is conducted in the above equation. The matrix N is a assemble of the outward normal vectors to the yield function and $\boldsymbol{K}$, a assemble of yield limits corresponding to outward normal vectors. The suffixes "o" and "e" mean the initial and elastic components of stresses. The bearing capacity analysis against the external force $\boldsymbol{F}$ can be formulated with a load factor α such as

$$s = \max \left| \alpha \left| \begin{array}{c} N^T \left\{ \begin{array}{c} \boldsymbol{\sigma}_o \\ \boldsymbol{m}_o \end{array} \right\} + \alpha N^T \left\{ \begin{array}{c} \boldsymbol{\sigma}^e \\ \boldsymbol{m}^e \end{array} \right\} \\ + N^T \left\{ \begin{array}{c} \overline{\boldsymbol{\sigma}}^r \\ \overline{\boldsymbol{m}}^r \end{array} \right\} - \boldsymbol{K} \leq \mathbf{o} \\ B^T \left\{ \begin{array}{c} \boldsymbol{\sigma}^e \\ \boldsymbol{m}^e \end{array} \right\} = \boldsymbol{F} \\ B^T \left\{ \begin{array}{c} \overline{\boldsymbol{\sigma}}^r \\ \overline{\boldsymbol{m}}^r \end{array} \right\} = \mathbf{o} \end{array} \right| \right| . \tag{2.4}$$

B is a matrix between the stress vector and the external force vector. The second and third equations describe the equilibrium equations on elastic and residual stresses, respectively. It is noted that the redistribution of stresses is considered with the residual stresses which are determined by solving the boundary value problem.

3 ULTIMATE BEARING CAPACITY OF FOUNDATION WITH FINITE RIGIDTY

The applicability of the proposed analysis is discussed by evaluating the ultimate bearing capacity of raft foundation with finite rigidity.

3.1 *Boundary Conditions and Soil Constants*

The bearing capacity analysis is conducted against a homogeneous load applied on raft foundation on clayey soils. Firstly, the accuracy of the proposed analysis is examined in comparison with the Hill's solution under the plane strain condition. The soils is modeled as the Mises material with the undrained shear strength. The soil constants employed in this analysis are exhibited in Table 1. Fig.1 shows the employed boundary condition and finite element mesh.

Table 1. Soil constants.

E	1000.0 kN/m^2	ν	0.33333
c_u	10.0 kN/m^2		

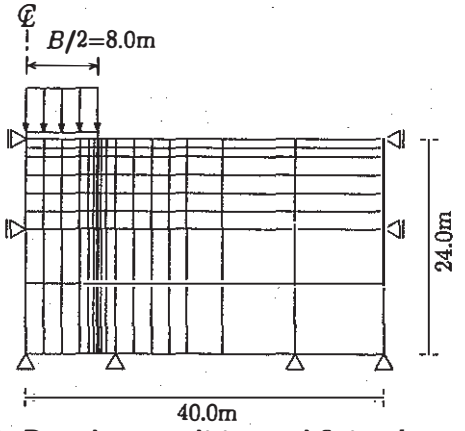

Fig.1 Boundary condition and finite element mesh.

3.2 *Effects of Mechanical Properties of Foundation*

The raft foundation is modeled as a beam and the effects of both bending rigidity, EI and limit bending moment, M_p on the bearing capacity is investigated. Fig.2 illustrates the relationship between the ultimate bearing capacity and limit bending moment M_p. The bending rigidity is set constant as $EI = 8.3 \times 10^0$, 8.3×10^8 kN·m^2. In the case of flexible foundation as $EI = 8.3 \times 10^0$ kN·m^2, the ultimate bearing capacity is obtained to be constant as $5.24c_u$ kN/m^2. It is close to the Hill's exact solution $(\pi + 2)c_u$ kN/m^2 and the accuracy of computation is comparatively well. In the case of rigid foundation as $EI = 8.3 \times 10^8$ kN·m^2, the ultimate bearing capacity is same as that of flexible foundation when the limit bending moment is high. However, it drastically reduces as the limit bending moment is lower than $M_p = 1.0 \times 10^4$ kN·m. It is lower than the Hill's solution and then,

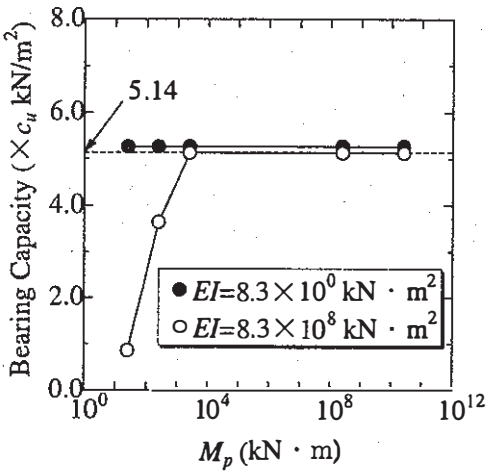

Fig.2 Relationship between ultimate bearing capacity and limit bending moment.

the ground is thought not to be failed. It is due to foundation failure because the stress tends to concentrate on the edge of foundation when the bending rigidity of foundation is high.

4 ULTIMATE BEARING CAPACITY OF REINFORCED SLOPE

The ultimate bearing capacity is assessed for raft foundation on the top of reinforced slope. The rigidity of foundation is set rigid as $EI = 8.3 \times 10^8$ kN·m^2. The boundary condition and finite element mesh are exhibited in Fig.3. The reinforcement is installed as shown in the figure and it is modeled as a truss element, the width of which is 0.01m. The material constants are shown in Table 2.

4.1 *Effect of Mechanical Properties of Reinforcement*

Fig.4 represents the relationship between the reinforcement effect and the tensile strength of reinforcements. The reinforcement effect is defined as the ratio of the ultimate bearing capacity to that of no reinforcements. The reinforcement rigidity is set constant as $E = 1.0 \times 10^2$, 1.0×10^{10} kN/m^2 in the figure. In both cases, the reinforcement effect is obtained higher with the tensile strength of reinforcements. However, it varies during the range of tensile strength σ_Y from 0 to 1.0×10^5 kN/m^2 and keeps constant even if the tensile strength of reinforcement is higher than 1.0×10^5 kN/m^2. It is noticed that there is a limited range of tensile strength on reinforcement to change the reinforcement effect largely. In these computations, the reinforcement effect is obtained

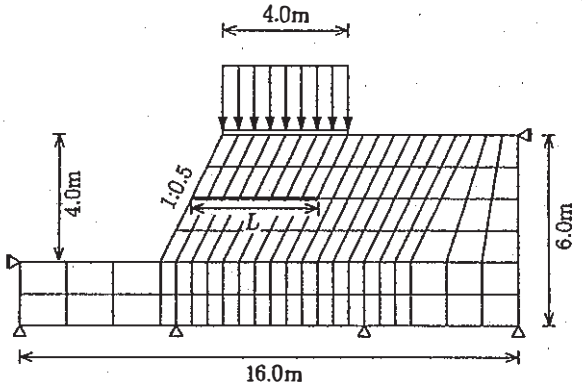

Fig.3 Boundary condition and finite element mesh.

Table 2. Soil constants.

E	1000.0 kN/m^2	ν	0.33333
γ_t	19.6 kN/m^3		
c	10.0 kN/m^2	ϕ	30.0°

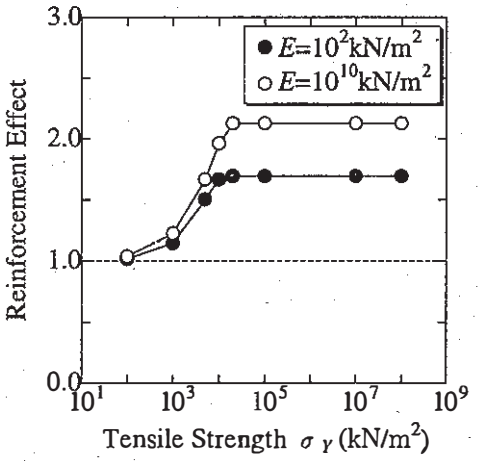

Fig.4 Reinforcement effect for tensile strength of reinforcements.

at most about twice.

Fig.5 exhibits the relationship between the reinforcement effect and reinforcement rigidity. It is found that the reinforcement effect can not be expected when the tensile strength of reinforcements is low. Then, the effect of reinforcement rigidity is negligible. In the case of the tensile strength as 1.0×10^5 kN/m^2, the reinforcement effect is large and varies depending on the tensile rigidity of reinforcements. The tendency of reinforcement effect with tensile rigidity is the same as that with tensile strength in Fig.4. There is observed a limited range of tensile rigidity where the reinforcement effect varies largely.

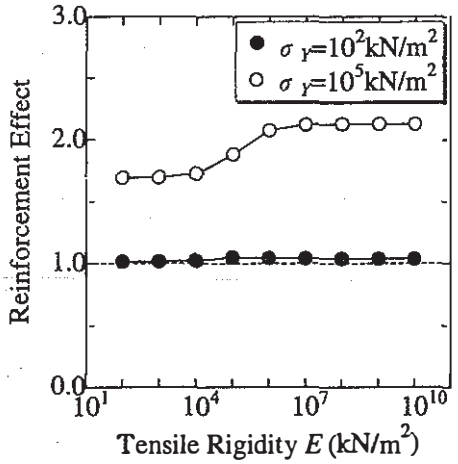

Fig.5 Reinforcement effect for tensile rigidity of reinforcement.

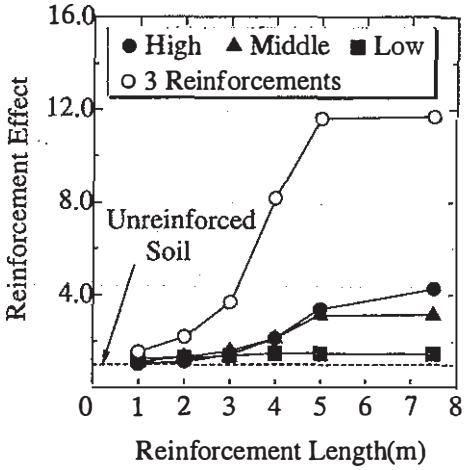

Fig.7 Reinforcement effect of configuration.

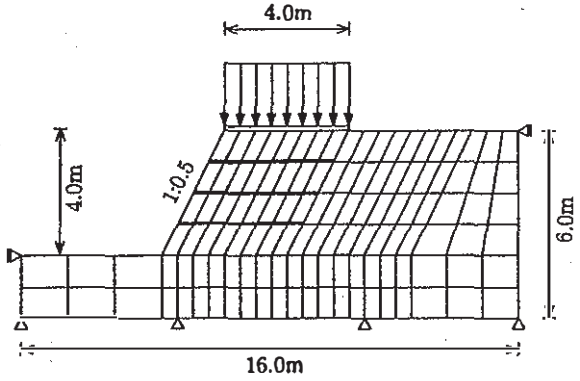

Fig.6 Boundary condition and finite element mesh.

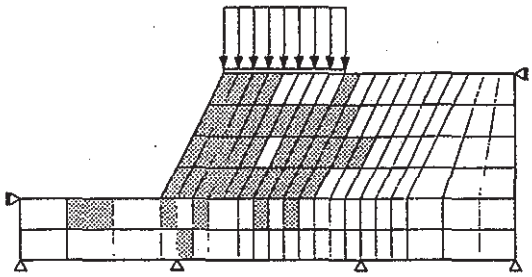

Fig.8 Yielded element distribution of slope without reinforcements.

4.2 *Reinforcement Configuration and Bearing Capacity*

The reinforcement effect on ultimate bearing capacity is also investigated for configuration of reinforcements. The employed finite element mesh is shown in Fig.6, the boundary condition of which is the same as Fig.3. The tensile strength and rigidity of reinforcements are set as $\sigma_Y = 1.0 \times 10^7$ kN/m^2 and $E = 1.0 \times 10^9$ kN/m^2. Firstly, the ultimate bearing capacity is computed for one reinforcement. The installed location of reinforcement is changed as low, middle and high as shown in Fig.6. The case of three reinforcements is also examined. The length of reinforcements is changed as 1.0, 2.0, 3.0, 4.0, 5.0 and 7.5m to investigate a reinforcement effect. The results are illustrated in Fig.7 all together. The reinforcement effect shows higher with the reinforcement length. In the case of one reinforcement, the reinforcement effect is obtained higher when it is installed at the upper location. However, it is much higher in the case of three reinforcements in comparison with the case of one reinforcement. On the reinforcement length, there is a threshold value that the reinforcement effect becomes constant even if the reinforcement length is longer. That is about 5.0m in each case in these cases. It indicates there exists an optimal length of reinforcements.

4.3 *Failure Mode and Axial Stress Distribution of Reinforcement*

The effect of reinforcement on failure mechanism is investigated with marking yielded elements obtained in stability analysis. Fig.8 shows the yielded element distribution of the slope without reinforcements. The Melan's theorem gives a lower bound on ultimate bearing capacity based on stress field and not on kinematic field. But, the shaded elements constitute a kind of failure zone as the same as the velocity field in the upper bound theorem.

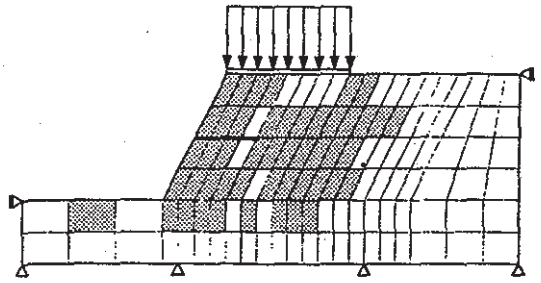

(a) Reinforcement length L=2.0m

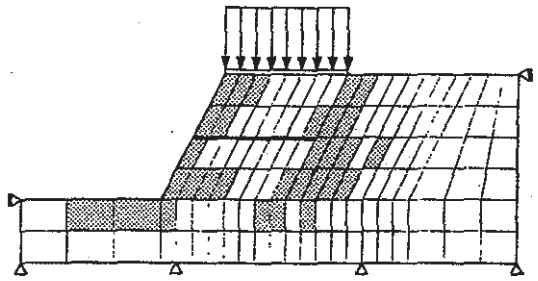

(b) Reinforcement length L=4.0m

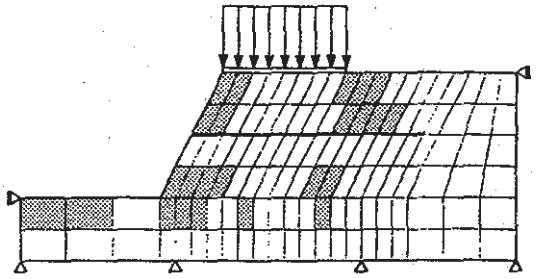

(c) Reinforcement length L=7.5m

Fig.9 Yielded element distribution in the case of one reinforcement.

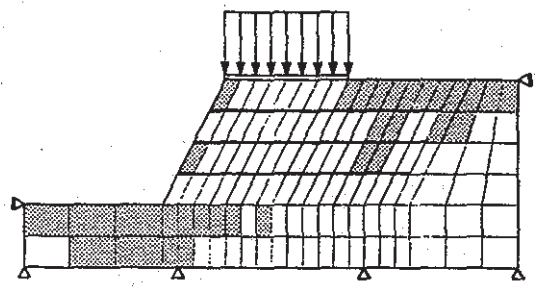

Fig.10 Yielded element distribution in the case of three reinforcements. (Reinforcement length L=7.5m)

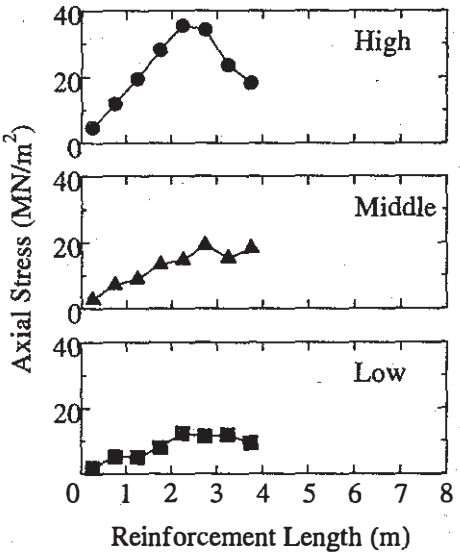

(a) Reinforcement length L=4.0m

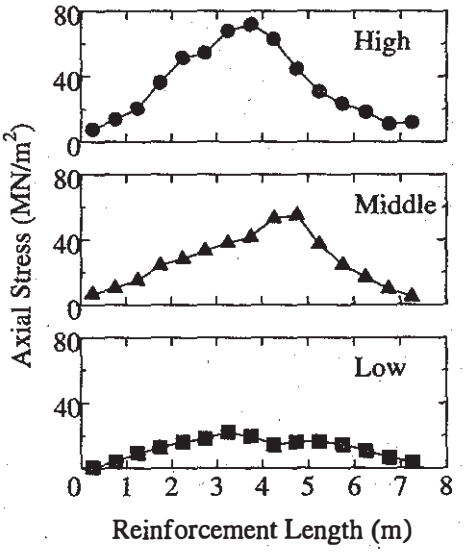

(b) Reinforcement length L=7.5m

Fig.11 Axial stress distribution of reinforcement at the limit state.

Fig.9 exhibits the yielded elements when one reinforcement is installed. The length of reinforcement is changed as 2.0, 4.0 and 7.5m. When the length of reinforcement is small, there is not so much difference in failure zone in comparison with the case of no reinforcement. But, it is found that the failure zone apparently expands with the length of reinforcement. This might be the reason why the ultimate bearing capacity gets higher. It is also

observed in Fig.10 which represents the yielded elements in the case of three reinforcements. It is noted that the failure zone is found to surround the installed reinforcements and the soil elements neighboring reinforcements stay within the elastic state. The axial stress of reinforcement at the limit state is exhibited in Fig.11 in the case of one reinforcement of $L = 4.0$ and 7.5m. They are obtained as the result of stress redistribution due to soil structure interaction. In the case of $L = 7.5$m, the peak axial stress is clearly observed at the upper and middle locations of reinforcements.

4.4 *Effect of Foundation Rigidity*

The ultimate bearing capacity is estimated for Fig. 3 with the reinforcement of $L = 7.5$m at the middle location in the slope. The rigidity of foundation on which the load is applied is modeled as $EI = 8.3 \times 10^0$ and 8.3×10^8 kN·m^2. These two might correspond to so-called flexible and rigid foundations. The computed results are obtained as Table 3. It is found there is a big difference in ultimate bearing capacity which is not predicted before computation. It indicates the importance of consideration on the rigidity of foundation. Fig.12 represents the axial stress distribution of the reinforcement. In the case of rigid foundation, there obtained high axial stress and the peak value.

Table 3. Comparison of ultimate bearing capacities for foundation rigidity.

	Flexible Foundation	Rigid Foundation
EI (kN/m^2)	8.3×10^0	8.3×10^8
q_f (kN/m^2)	64.9	392.8

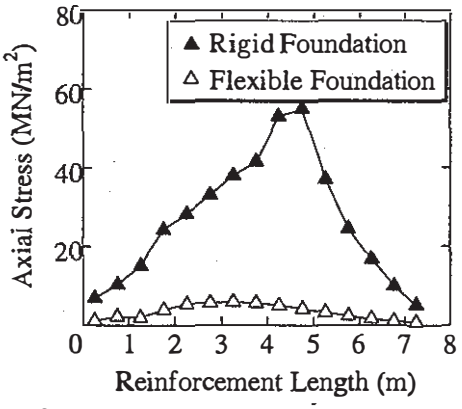

Fig.12 Comparison of axial stress distributions of reinforcement for foundation rigidity.

5 CONCLUSIONS

The followings are concluded in this study.

1. The stability analysis of soil structure system was proposed and the applicability of it was examined through some numerical analyses.

2. The ultimate bearing capacity of raft foundation was investigated for the rigidity and limit bending moment of foundation. The ultimate bearing capacity was shown to vary with mechanical properties of foundation. When the limit bending moment of foundation was low, the ultimate bearing capacity drastically decreased. It is why the foundation fails by itself. In the case of clayey soils, there was little difference in the ultimate bearing capacity with the foundation rigidity.

3. The ultimate bearing capacity of foundation on the top of reinforced slope was estimated and the reinforcement effect on the ultimate bearing capacity was investigated by parametric studies. The ultimate bearing capacity was shown to increase with the tensile strength of reinforcement, but, vary in the limit range of tensile strength, $\sigma_Y = 0 \sim 1.0 \times 10^5$ kN/m^2.

The effect of reinforcement configuration on the ultimate bearing capacity was also investigated and the reinforcement mechanism was discussed with the yielded elements obtained in the stability analysis. It was found that the yielded area surrounded installed reinforcements and the soils neighboring reinforcements stayed within the elastic state. The axial stress distribution of reinforcements were also illustrated.

REFERENCES

Koiter, W. T. (1960). General theorems for elastic plastic solids, *Progress of Solid Mechanics*, Chap.6, Vol.2, North Holland Press.

Maier, G. (1969). Shakedown theory in perfect elastoplasticity with associated and nonassociated flow-laws: a finite element linear programming approach, *Meccanica*, Vol.4, No.3, pp.1–11.

Maier, G. (1977). Shakedown Analysis, *Proc. of the NATO Advanced Study Institute*, Engineering Plasticity by Mathematical Programming, Chap.6, pp.107–134.